

## Brillouin scattering determination of the surface acoustic wave velocity in $\text{In}_x\text{Ga}_{1-x}\text{N}$ : A probe into the elastic constants

R. J. Jiménez-Riobóo, R. Cuscó, R. Oliva, N. Domènech-Amador, C. Prieto et al.

Citation: *Appl. Phys. Lett.* **101**, 062103 (2012); doi: 10.1063/1.4744961

View online: <http://dx.doi.org/10.1063/1.4744961>

View Table of Contents: <http://apl.aip.org/resource/1/APPLAB/v101/i6>

Published by the [American Institute of Physics](http://www.aip.org).

### Additional information on *Appl. Phys. Lett.*

Journal Homepage: <http://apl.aip.org/>

Journal Information: [http://apl.aip.org/about/about\\_the\\_journal](http://apl.aip.org/about/about_the_journal)

Top downloads: [http://apl.aip.org/features/most\\_downloaded](http://apl.aip.org/features/most_downloaded)

Information for Authors: <http://apl.aip.org/authors>

## ADVERTISEMENT

**minus k<sup>®</sup> TECHNOLOGY** *20 years* **Improve your Images with Minus K's**  
**Negative-Stiffness Vibration Isolation**

**Workstations & Optical Tables** **Bench Top Isolators** **Without Minus K** **With Minus K**

**Custom Applications** **Multi Isolator Systems** **Floor Platforms**



The advertisement features several images and logos. On the left, there are images of workstations and optical tables. In the center, there are images of bench top isolators and multi isolator systems. On the right, there are images of floor platforms. The central part of the advertisement shows two side-by-side topography scans of a surface. The left scan is labeled 'Without Minus K' and shows a very noisy, grainy surface. The right scan is labeled 'With Minus K' and shows a much smoother surface. The scans are labeled 'Topography - Scan forward' and have axes labeled '5µm' and '2.5µm'. The logos for NASA, ESA, JPL, and JWST are also visible.

# Brillouin scattering determination of the surface acoustic wave velocity in $\text{In}_x\text{Ga}_{1-x}\text{N}$ : A probe into the elastic constants

R. J. Jiménez-Riobóo,<sup>1</sup> R. Cuscó,<sup>2</sup> R. Oliva,<sup>2</sup> N. Domènech-Amador,<sup>2</sup> C. Prieto,<sup>1</sup> J. Ibáñez,<sup>2</sup> C. Boney,<sup>3</sup> A. Bensaoula,<sup>3</sup> and L. Artús<sup>2</sup>

<sup>1</sup>Instituto de Ciencia de Materiales de Madrid, CSIC, Cantoblanco, Madrid 28049, Spain

<sup>2</sup>Institut Jaume Almera, Consell Superior d'Investigacions Científiques (CSIC), Lluís Solé i Sabarís s.n., 08028 Barcelona, Catalonia, Spain

<sup>3</sup>Department of Physics, University of Houston, 4800 Calhoun, Houston, Texas 77004, USA

(Received 15 June 2012; accepted 26 July 2012; published online 8 August 2012)

We have determined the surface acoustic wave velocity in  $\text{In}_x\text{Ga}_{1-x}\text{N}$  layers for  $0.34 < x < 0.75$  by means of high resolution Brillouin spectroscopy. The sagittal dependence of the surface acoustic velocity has been analyzed by comparing the experimental results with theoretical simulations based on the Green's function formalism. We find the best agreement with our data when the bowing parameters for the elastic constants recently reported from density functional theory calculations are taken into account. The dependence of the surface acoustic wave velocity on alloy composition is given. © 2012 American Institute of Physics. [<http://dx.doi.org/10.1063/1.4744961>]

Group III nitride-based materials have important applications in optoelectronics and high-power/high-temperature electronics. Alloying in this material system offers a great flexibility for tailoring the physical properties of the active layers of electronic devices. GaN-based heterostructure field effect transistors (HFET) with InN-containing barrier/channel layers are the subject of intense current research.<sup>1</sup> The piezoelectric properties of group III nitrides also make these materials very attractive for surface acoustic wave (SAW) device applications. AlN is one of the most suitable materials for high-frequency filters, duplexers, and resonators because of its high SAW velocity and its insulating nature.<sup>2,3</sup> On the other hand, GaN-based SAW delay-line oscillators have shown their potential as visible-blind remote UV sensors.<sup>4</sup> Given that the bandgap of  $\text{In}_x\text{Ga}_{1-x}\text{N}$  can be tuned from 0.64 eV ( $x = 1$ ) to 3.4 eV ( $x = 0$ )<sup>5</sup> and that the alloy exhibits a higher electromechanical coupling than GaN, InGaN-based SAW devices are good candidates for sensitive visible light sensors.

Despite the enormous technological interest of group III-nitride alloys for piezoelectric applications, there is relatively little information about the elastic properties of these materials. The knowledge of the elastic constants of  $\text{In}_x\text{Ga}_{1-x}\text{N}$  is necessary to model and optimize the design of InGaN-based piezoelectric and strained layer devices. Brillouin scattering is a powerful technique for an accurate determination of the elastic constants.<sup>6,7</sup> Whereas Brillouin scattering studies have been reported for GaN (Refs. 8–10) and InN (Ref. 11), no experimental determinations of the elastic constants of wurtzite  $\text{In}_x\text{Ga}_{1-x}\text{N}$  are available so far. Thus, a Vegard-like linear interpolation between the values of the binary compounds is usually assumed when strain analysis is required for the InGaN alloy.<sup>12,13</sup>

It is well known that In has a tendency to segregation and clustering in nitride alloys, and this may have a strong impact on their optical emission<sup>14,15</sup> and piezoelectric<sup>16</sup> properties. Recently, *ab initio* calculations of the dependence of the elastic constants on composition have been reported for  $\text{In}_x\text{Ga}_{1-x}\text{N}$  and  $\text{In}_x\text{Al}_{1-x}\text{N}$  wurtzite alloys.<sup>17</sup> These calcu-

lations reveal significant sublinear deviations for some of the elastic constants of  $\text{In}_x\text{Ga}_{1-x}\text{N}$ , and considerable differences are found if In clustering is taken into account in the supercell model. A comparison of these theoretical predictions with experimental data has not been reported so far.

In this letter, we present a high resolution Brillouin scattering (HRBS) study of the SAW velocity in  $\text{In}_x\text{Ga}_{1-x}\text{N}$  alloys with In compositions ranging from  $x = 0.34$  to  $x = 0.75$ . The sagittal dependence of the observed Rayleigh and Sezawa modes is analyzed by comparing with simulations based on the Green's function formalism for SAW propagation.<sup>18</sup>

The InGaN epilayers used in this work (see Table I) were grown by plasma-assisted molecular beam epitaxy on a 4- $\mu\text{m}$  thick GaN template on (0001)-sapphire substrates. Growth details and characterization of these samples have been published elsewhere.<sup>19</sup> HRBS experiments were performed in backscattering geometry for different sagittal angles using the  $\lambda_0 = 514.5$  nm excitation wavelength. A description of the experimental set-up can be found in Ref. 20. The studied samples have In compositions above  $x = 0.34$ . For these compositions, the strong optical absorption prevents the signal of the bulk acoustic phonons to be detected and therefore the scattering signal from the SAW can be measured. It was not possible to study samples with

TABLE I. Characteristics of the  $\text{In}_x\text{Ga}_{1-x}\text{N}$  samples and their respective SAW velocity determined from the Brillouin measurements. The SAW velocity values were determined by averaging the measurements with  $kh > 10$ , for which the influence of the substrate is negligible. Here,  $h$  is the thickness of the  $\text{In}_x\text{Ga}_{1-x}\text{N}$  layer and  $k$  is the acoustic scattering wave vector (see text).

Sample	In content	$h$ (nm)	$v_{\text{SAW}}$ ( $\text{ms}^{-1}$ )
A1010	0.34	710	3161
A1018	0.42	710	3114
A1035	0.44	560	3057
A1177	0.68	500	2880
A1182	0.75	500	2754

less In content because in the transparency regime the strong luminescence background and the dominance of the substrate modes precluded the observation of the SAW peaks.

Figure 1 shows representative Brillouin spectra obtained from sample A1182 for different values of the sagittal angle  $\alpha$ , which is defined by the incident laser beam and the normal to the film surface. Since we are measuring opaque samples, contribution to inelastic light scattering is due to surface corrugation produced by the propagation of SAW (ripple effect). This ripple mechanism accounts for most of the scattered light giving rise to surface Rayleigh phonons and makes it possible the presence of guided waves in addition to the Rayleigh wave when the transverse velocity of phonons in the film is smaller than that of the substrate.<sup>6,7</sup> This guided waves, which have a higher energy than the Rayleigh modes, are known as Sezawa modes. Thus, the most intense peak is assigned to the Rayleigh mode and the weaker peaks at higher energies are assigned to the Sezawa modes. Both peaks shift to higher frequencies for increasing  $\alpha$ , which reflects the increase in the component along the surface of the acoustic scattering wave vector  $k = 4\pi\sin\alpha/\lambda_0$ . The SAW velocity can be directly obtained from the Rayleigh peak frequency  $\nu_R$  as  $v_{\text{SAW}} = 2\pi\nu_R/k$ . Lorentzian line shape fits were carried out to extract the  $\nu_R$  values from the spectra. Brillouin spectra taken at different sagittal angles  $\alpha$  (from  $\alpha = 30^\circ$  to  $\alpha = 75^\circ$  at  $5^\circ$  steps) have allowed us to obtain  $v_{\text{SAW}}$  values for a range of  $kh$  values  $6 < kh < 13$ .

In thin films, the substrate can affect the  $v_{\text{SAW}}$  of the layer depending on the  $kh$  value. This is illustrated by the calculated curves shown in Fig. 2, where it can be seen that to measure the intrinsic  $v_{\text{SAW}}$  of the thin-film material  $kh$  values in the flat, asymptotic region of the curves must be reached. Given the layer thickness of the samples used in this study (see Table I), the sagittal angles used in the experiments yield  $kh$  values that are high enough to render the Rayleigh SAW velocity nearly independent of the substrate. By contrast, in this range of  $kh$  values the Sezawa SAW velocity still shows a marked dependence on the sagittal angle  $\alpha$ .

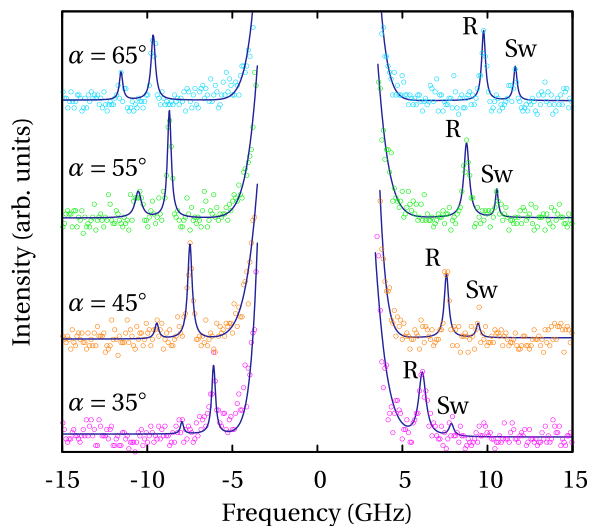


FIG. 1. Brillouin spectra of sample A1182 ( $x = 0.75$ ) obtained at different sagittal angles. Solid lines are Lorentzian line shape fits to the spectra. The Rayleigh and Sezawa peaks are labeled as R and Sw, respectively.

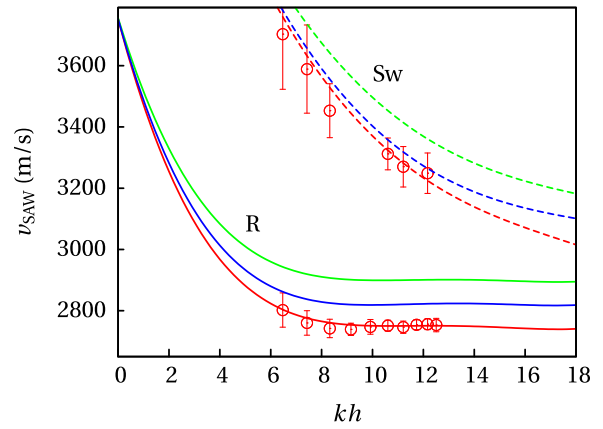


FIG. 2. Surface acoustic wave velocities as a function of  $kh$  for an  $\text{In}_x\text{Ga}_{1-x}\text{N}$  layer with  $x = 0.75$ , as obtained from the Green's function simulations using different interpolation schemes for the elastic constants: Vegard-like linear interpolation (green lines), *ab initio* results for a uniform alloy (blue lines), *idem* for a clustered alloy (red lines). The circles represent the experimental Brillouin data. R and Sw stand for Rayleigh and Sezawa modes, respectively.

The sagittal dependence of the scattered light intensity for  $\text{In}_x\text{Ga}_{1-x}\text{N}$  thin films on GaN/sapphire was simulated using the Green's function formalism developed by Zhang *et al.*<sup>18</sup> The density used for  $\text{In}_x\text{Ga}_{1-x}\text{N}$  was interpolated from those of InN ( $6.81 \text{ g cm}^{-3}$ ) and GaN ( $6.15 \text{ g cm}^{-3}$ ),<sup>5</sup> assuming a linear dependence of the lattice parameters with composition (Vegard's law). Three different sets of elastic constants were considered in the simulations: (i) Vegard-like linear interpolation between the elastic constants of GaN and InN, (ii) quadratic parametrization of the elastic constants calculated using *ab initio* methods<sup>17</sup> with the bowing parameter corresponding to a uniform distribution of In atoms, and (iii) *idem* with the bowing parameter corresponding to a clustered distribution of In atoms. In the last two cases, the values of the elastic constants are obtained as a function of the In concentration using

$$c_{ij}^{\text{InGa}}(x) = (1-x)c_{ij}^{\text{GaN}} + xc_{ij}^{\text{InN}} - b_{ij}x(1-x) \quad (1)$$

with the bowing parameters  $b_{ij}$  reported in Ref. 17 (see Table II). In all cases, the elastic constants for the end member compounds were taken from previous Brillouin studies.<sup>9-11</sup> As can be seen in Table II, substantial values of the bowing parameters for the  $c_{11}$  and  $c_{33}$  elastic constants are obtained

TABLE II. Elastic constants for the end-member compounds (in GPa) and bowing parameters used in the  $\text{In}_x\text{Ga}_{1-x}\text{N}$  SAW simulations. Note that in hexagonal symmetry crystals  $c_{66} = (c_{11} - c_{12})/2$ .

	$c_{11}$	$c_{12}$	$c_{13}$	$c_{33}$	$c_{44}$
GaN <sup>a</sup>	376.4	137.2	114.0	406.8	94.6
InN <sup>b</sup>	222.7	112.1	107.5	258	48.5
$b$ (uniform) <sup>c</sup>	60	14	-4	71	16
$b$ (clustered) <sup>c</sup>	100	43	-4.5	-1	35

<sup>a</sup>Reference 10. The  $c_{13}$  value, which was not determined in Ref. 10, has been taken from Ref. 9.

<sup>b</sup>Reference 11.

<sup>c</sup>Reference 17.



from the *ab initio* calculations when a uniform In distribution is assumed, which imply a significant sublinear dependence on composition of these elastic constants. On the other hand, if In clustering is taken into account, the greatest bowing is exhibited by the  $c_{11}$ ,  $c_{12}$ , and  $c_{44}$  elastic constants. The different composition dependence of the elastic constants in each case results in different values of the  $v_{\text{SAW}}$ .

The Rayleigh (solid lines) and Sezawa (dashed lines) acoustic wave velocities simulated using the three different sets of alloy elastic constants mentioned above are plotted in Fig. 2 for an In concentration of  $x = 0.75$ . In the same figure, we have plotted the Rayleigh and Sezawa acoustic wave velocities measured at different  $kh$  values in sample A1182, which as shown in Ref. 19 corresponds to a fully relaxed  $\text{In}_{0.75}\text{Ga}_{0.25}\text{N}$  epilayer. As can be seen in Fig. 2, the simulation with the linearly interpolated elastic constants (case *i*) overestimates the SAW velocity by about 10% (green lines). If the set of constants obtained for the homogeneous alloy from *ab-initio* calculations (case *ii*) is considered in the simulations, the resulting SAW velocities (blue lines) are in better agreement with the experimental points, although they still overestimate the measured velocity. Finally, if we consider the elastic constants calculated for clustered alloys (case *iii*), an excellent agreement with the experimental velocities of both Rayleigh and Sezawa modes is obtained (red line). Although the full determination of the elastic constants from the  $v_{\text{SAW}}$  measurements is not possible, this result suggests that a significant degree of bowing in the composition dependence of the elastic constants, which may be related with an inhomogeneous In distribution,<sup>17</sup> has to be considered. Similar quality fits are obtained for all the alloy compositions studied.

As can be seen in Fig. 2, for the  $kh$  values used in this study the Rayleigh acoustic wave velocity is nearly independent of the substrate. By performing HRBS experiments at high  $kh$  values on different alloy composition samples, the composition dependence of the intrinsic SAW velocity was obtained and it is plotted in Fig. 3. In contrast with the linear dependence on composition of the sound velocity found in  $\text{Al}_x\text{Ga}_{1-x}\text{N}$  (Ref. 10), the SAW velocity in  $\text{In}_x\text{Ga}_{1-x}\text{N}$  exhibits a noticeable bowing. A good agreement is found between the measured  $v_{\text{SAW}}$  values and the composition dependence obtained from the simulations using the set of elastic constants of case *iii* (solid line in Fig. 3). Although, as reported in Ref. 19, a residual strain is present in the samples with In concentration between 0.34 and 0.44, the results shown in Fig. 3 indicate that this has not a significant influence on the measured SAW velocities, which are well described by the simulations using the elastic constants given by Eq. (1) throughout all the composition range. Whereas the compressive strain in the  $\text{In}_x\text{Ga}_{1-x}\text{N}$  layer induces an increase in the elastic constants via nonlinear elasticity effects<sup>21</sup> and tends to increase the sound velocity, the concomitant reduction of the unit cell volume results in an increase of the density and hence lowers the sound velocity. These compensating effects, together with a possible strain relaxation towards the surface, may explain the observation that the  $v_{\text{SAW}}$  values measured in the layers with residual strain are in good agreement with the composition dependence of  $v_{\text{SAW}}$  calculated for relaxed samples.

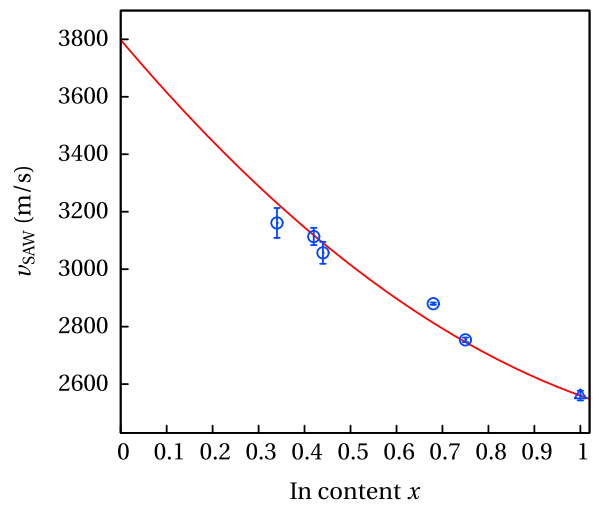


FIG. 3. Composition dependence of the surface acoustic velocity of  $\text{In}_x\text{Ga}_{1-x}\text{N}$ . Circles are the experimental values measured in this work. The triangle represents the measured  $v_{\text{SAW}}$  value for InN reported in Ref. 11. The solid line is the simulated  $v_{\text{SAW}}$  considering the set of elastic constants of case *iii* (see text), which take into account the effect of In clustering in the alloy.

In summary, we have performed an experimental determination of the SAW velocity of the  $\text{In}_x\text{Ga}_{1-x}\text{N}$  alloy by means of HRBS measurements. The sagittal dependence of the SAW velocities we find for both Rayleigh and Sezawa modes is well described by a Green's function simulation of the scattered intensity only when a significant bowing is included in the composition dependence of the elastic constants, as given by *ab initio* calculations on clustered supercells. The bowing values of the elastic constants required to explain the  $v_{\text{SAW}}$  values for the different InGaN alloys suggest that some degree of inhomogeneity in In distribution may exist in these alloys. Because of the relatively large layer thicknesses of the studied samples, the Rayleigh SAW velocity was found to be independent of the sagittal angles used in the experiments, and the intrinsic SAW velocity of  $\text{In}_x\text{Ga}_{1-x}\text{N}$  alloys could be determined from the HRBS measurements. The good agreement of the Green's function simulations with both the composition and the sagittal-angle dependence of  $v_{\text{SAW}}$  obtained from Brillouin measurements reinforces the knowledge gained from these measurements on the elastic properties of the  $\text{In}_x\text{Ga}_{1-x}\text{N}$  alloys.

This work has been partially supported by the Spanish Ministry under Grants MAT2010-16116 and MAT2009-08786.

- <sup>1</sup>J. Liberis, I. Matulionienė, A. Matulionis, E. Šermukšnis, J. Xie, J. H. Leach, and H. Morkoç, *Phys. Status Solidi A* **206**, 1385 (2009).
- <sup>2</sup>O. Ambacher, *J. Phys. D* **31**, 2653 (1998).
- <sup>3</sup>Y. Takagaki, P. Santos, E. Wiebicke, O. Brandt, H. Schonherr, and K. Ploog, *Appl. Phys. Lett.* **81**, 2538 (2002).
- <sup>4</sup>D. Ciplys, R. Rimeika, M. S. Shur, S. Rumyantsev, R. Gaska, A. Sereika, J. Yang, and M. A. Khan, *Appl. Phys. Lett.* **80**, 2020 (2002).
- <sup>5</sup>J. Wu, *J. Appl. Phys.* **106**, 011101 (2009).
- <sup>6</sup>J. R. Sandercock, *Light Scattering in Solids III, Topics in Applied Physics Vol. 51*, edited by M. Cardona and G. Güntherodt (Springer-Verlag, Berlin, 1982).
- <sup>7</sup>P. Mutti, C. E. Bottani, G. Ghisloti, M. Beghi, G. A. D. Briggs, and J. R. Sandercock, *Advanced in Acoustic Microscopy*, edited by A. Briggs (Plenum, New York, 1995), Vol. 1.
- <sup>8</sup>A. Polian, M. Grimsditch, and I. Grzegory, *J. Appl. Phys.* **79**, 3343 (1996).

- <sup>9</sup>M. Yamaguchi, T. Yagi, T. Sota, T. Deguchi, K. Shimada, and S. Nakamura, *J. Appl. Phys.* **85**, 8502 (1999).
- <sup>10</sup>R. J. Jiménez Riobóo, E. Rodríguez-Cañas, M. Vila, C. Prieto, F. Calle, T. Palacios, M. A. Sánchez, F. Omnès, O. Ambacher, B. Assouar, and O. Elmazria, *J. Appl. Phys.* **92**, 6868 (2002).
- <sup>11</sup>R. J. Jiménez-Riobóo, R. Cuscó, N. Domènech-Amador, C. Prieto, T. Yamaguchi, Y. Nanishi, and L. Artús, *Phys. Status Solidi (RRL)* **6**, 256 (2012).
- <sup>12</sup>S. Pereira, M. R. Correia, T. Monteiro, E. Pereira, E. Alves, A. D. Sequeira, and N. Franco, *Appl. Phys. Lett.* **78**, 2137 (2001).
- <sup>13</sup>M. Winkelkemper, A. Schliwa, and D. Bimberg, *Phys. Rev. B* **74**, 155322 (2006).
- <sup>14</sup>S. Chichibu, T. Azuhata, T. Sota, and S. Nakamura, *Appl. Phys. Lett.* **70**, 2822 (1997).
- <sup>15</sup>K. O'Donnell, R. Martin, and P. Middleton, *Phys. Rev. Lett.* **82**, 237 (1999).
- <sup>16</sup>A. Al-Yacoub, L. Bellaiche, and S. Wei, *Phys. Rev. Lett.* **89**, 057601 (2002).
- <sup>17</sup>S. P. Łepkowski and I. Gorczyca, *Phys. Rev. B* **83**, 203201 (2011).
- <sup>18</sup>X. Zhang, J. D. Comins, A. G. Every, P. R. Stoddart, W. Pang, and T. E. Derry, *Phys. Rev. B* **58**, 13677 (1998).
- <sup>19</sup>R. Oliva, J. Ibáñez, R. Cuscó, R. Kudrawiec, J. Serafinczuk, O. Martínez, J. Jiménez, M. Henini, C. Boney, A. Bensaoula, and L. Artús, *J. Appl. Phys.* **111**, 063502 (2012).
- <sup>20</sup>R. J. Jiménez Riobóo, M. García-Hernández, C. Prieto, J. J. Fuentes-Gallego, E. Blanco, and M. Ramírez del Solar, *J. Appl. Phys.* **81**, 7739 (1997).
- <sup>21</sup>S. P. Łepkowski, *Phys. Rev. B* **75**, 195303 (2007).